ISSN 0021-3640, JETP Letters, 2019, Vol. 110, No. 3, pp. 160–165. © Pleiades Publishing, Inc., 2019.
Russian Text © The Author(s), 2019, published in Pis'ma v Zhurnal Eksperimental'noi i Teoreticheskoi Fiziki, 2019, Vol. 110, No. 3, pp. 149–154.

CONDENSED MATTER

Ferromagnetic Resonance and the Dynamics of the Magnetic Moment in a "Josephson Junction–Nanomagnet" System

Yu. M. Shukrinov[a, b, *], M. Nashaat[a, c], I. R. Rahmonov[a, d], and K. V. Kulikov[a]

[a] *Joint Institute for Nuclear Research, Dubna, Moscow region, 141980 Russia*

[b] *Dubna State University, Dubna, Moscow region, 141980 Russia*

[c] *Department of Physics, Cairo University, 12613 Cairo, Egypt*

[d] *Umarov Physical and Technical Institute, Academy of Sciences of the Republic of Tajikistan, Dushanbe, 734063 Tajikistan*

**e-mail: shukrinv@theor.jinr.ru*

Received May 7, 2019; revised June 11, 2019; accepted June 11, 2019

The dynamics of a nanomagnet coupled to a Josephson junction has been studied. Although a magnetic field induced by the superconducting current in the Josephson junction is very weak, an applied voltage can generate the nonlinear dynamics of the nanomagnet, which gives a number of interesting phenomena. It has been shown that a ferromagnetic resonance can occur when the frequency of Josephson oscillations becomes equal to the eigenfrequency of the magnetic system. It has been demonstrated that the easy axis of the nanomagnet is reoriented at an increase in the Josephson-to-magnetic energy ratio, as well as in the coupling parameter between the Josephson current and the magnetic moment and in the frequency of Josephson oscillations. It has been shown that a current pulse can turn the magnetic moment of the nanomagnet, which opens new prospects for the application of this system in superconducting spintronics.

DOI: 10.1134/S002136401915013X

Models describing the interaction between the superconducting current and magnetic moment in various superconductor–ferromagnet–superconductor structures, which are important for a number of problems of superconducting spintronics, have recently attracted great attention [1–4]. The authors of [1] emphasize that studies in spintronics allow understanding fundamental spin-depending phenomena, as well as developing applications for computer technologies. In particular, the superconductivity control of the magnetic state opens new possibilities for developing ultrafast cryogenic memory.

Coupling between the Josephson junction and magnet located very close to each other can be due to different mechanisms. In particular, the Rashba spin–orbit coupling results in the phase shift in the Josephson junction proportional to the magnetic moment in the barrier. As a result, the so-called φ_0 junction appears, where the phase difference is directly coupled to the magnetic moment in the barrier [5, 6], which provides unique possibilities for controlling the magnetic properties of the barrier by the superconducting current and, in turn, the influence of the magnetic moment of the barrier on the Josephson current [1–11]. The possibility of the reorientation of the easy axis in the presence of the spin–orbit coupling was reported in [3, 6]. Under the assumption that the easy axis is initially oriented along the z axis, it was shown that the superconducting current makes the stable orientation of the magnetization be directed between the z and y axes depending on the parameters of the system. The results obtained open the possibility of development of an efficient method for determining the spin–orbit coupling in ferromagnetic metals. The development of new efficient methods for the flip of the magnetic moment, in particular, by applying a current pulse is of great interest for various applications. Such studies will allow fabricating memory elements and other elements for quantum computers, as well as establishing the foundations for the development of new devices for superconducting spintronics.

Another coupling mechanism was studied in [11], whose authors considered the electromagnetic interaction of the nanomagnet with the Josephson junction at which the magnetic field of the nanomagnet changes the superconducting current flowing through the junction, whereas the magnetic field generated in the Josephson junction acts the magnetic moment of the nanomagnet. The structure considered in [1] differs from that studied in [6] in geometry, character of interaction, and finite normal weak coupling resistance, which was taken into account in [1] within the resistively shunted junction (RSJ) model [13]. The model with the pure electromagnetic interaction is

attractive because of the absence of unknown parameters, which is important for its experimental implementation [11].

In this work, we study the dynamics of the nanomagnet coupled to the Josephson junction. We show that the ferromagnetic resonance is manifested on the dependence of the maximum amplitude of oscillations of the nanomagnet on the voltage applied to the Josephson junction and the easy axis of the nanomagnet is reoriented under the variation of the parameters of the system. To demonstrate the prospects of the application of the studied system, we show the possibility of the flip of the magnetic moment of the nanomagnet by a current pulse.

The schematic of the considered system consisting of a Josephson junction and a nanomagnet coupled to it is shown in Fig. 1. The Josephson junction has the length l and the nanomagnet is located at the distance a from the center of the Josephson junction. It is assumed that the easy axis of the nanomagnet is directed along the y axis and the voltage V is applied to the Josephson junction.

The dynamics of the magnetic moment is described by the Landau–Lifshitz–Gilbert equations [14, 15]; in dimensionless quantities, these equations have the form

$$\frac{dm_x}{dt} = \frac{\Omega_F}{(1+m^2\alpha^2)}\Big[h_y\left(m_z - \alpha m_x m_y\right) - h_z\left(\alpha m_x m_z + m_y\right) + \alpha h_x\left(m_y^2 + m_z^2\right)\Big],$$

$$\frac{dm_y}{dt} = \frac{\Omega_F}{(1+m^2\alpha^2)}\Big[-h_x\left(\alpha m_x m_y + m_z\right) + h_z\left(m_x - \alpha m_y m_z\right) + \alpha h_y\left(m_x^2 + m_z^2\right)\Big], \quad (1)$$

$$\frac{dm_z}{dt} = \frac{\Omega_F}{1+m^2\alpha^2 + \Omega_F\alpha\epsilon k(m_x^2+m_y^2)} \times \Big[\alpha\epsilon[\sin(Vt - km_z) + V]\left(m_x^2 + m_y^2\right) - h_y\left(m_x + \alpha m_y m_z\right) + h_x\left(m_y - \alpha m_x m_z\right)\Big].$$

Here, $m_i = M_i/M_s$ is the normalized component of the magnetic moment, where M_s is the saturation magnetic moment; $\Omega_F = \omega_F/\omega_c$ is the normalized frequency of the ferromagnetic resonance, where $\omega_c = 2eRI_c/\hbar$ and I_c is the critical current; $k = \frac{2\pi}{\Phi_0}\frac{\mu_0 M_s l}{a\sqrt{l^2+a^2}}$, where $a = |\mathbf{r}_M|$ and Φ_0 is the magnetic flux quantum; m is the absolute value of the magnetic moment; α is the Gilbert damping parameter; the time t is measured in units of ω_c^{-1}; and the voltage V is measured in units of $\hbar\omega_c/(2e)$. The components of the dimensionless effective magnetic field h_i are given by the expression [11]

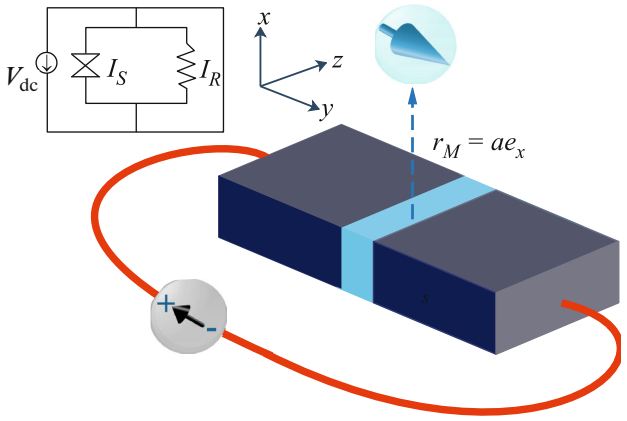

Fig. 1. (Color online) Schematic of the considered system with the equivalent electric circuit.

$$h_x = 0,$$
$$h_y = m_y, \quad (2)$$
$$h_z = \epsilon[\sin(Vt - km_z) + V] - \epsilon k\frac{dm_z}{dt}.$$

Here, $\epsilon = Gk$, where $G = \epsilon_J/K_{anV}$, $\epsilon_J = \Phi_0 I_c/(2\pi)$ is the Josephson energy, v is the volume of the nanomagnet, and K_{an} is the magnetic anisotropy constant. The components of the effective magnetic fields are measured in units of $H_F = \omega_F/\gamma$, where γ is the gyromagnetic ratio.

Josephson oscillations in the Josephson junction excite the precession of the magnetic moment of the nanomagnet, which leads to the ferromagnetic resonance when the precession frequency becomes equal to the eigenfrequency Ω_F of the magnetic system. To describe the resonance, the system of Eqs. (1) was solved by the Gauss–Legendre method [12] at a fixed voltage V. As a result, we determined the time dependences of the magnetic moment components and calculated the maximum amplitude of oscillations of the magnetic moment component in the time domain for each given voltage.

Figure 2a shows the calculated maximum amplitude of oscillations m_z^{max} as a function of the voltage V across the Josephson junction at $\Omega_F = 0.5$ and two damping parameters $\alpha = 0.001$ and 0.3. In the chosen normalization, $V = \Omega_J$; for this reason, a ferromagnetic resonance peak is observed at the voltage corresponding to the frequency of Josephson oscillations $\Omega_J = 0.5$. The result for m_x^{max} is qualitatively the same and is not presented. An enhancement of damping in the system leads to the broadening of the resonance and its shift toward lower frequencies, which is seen in Fig. 2a at

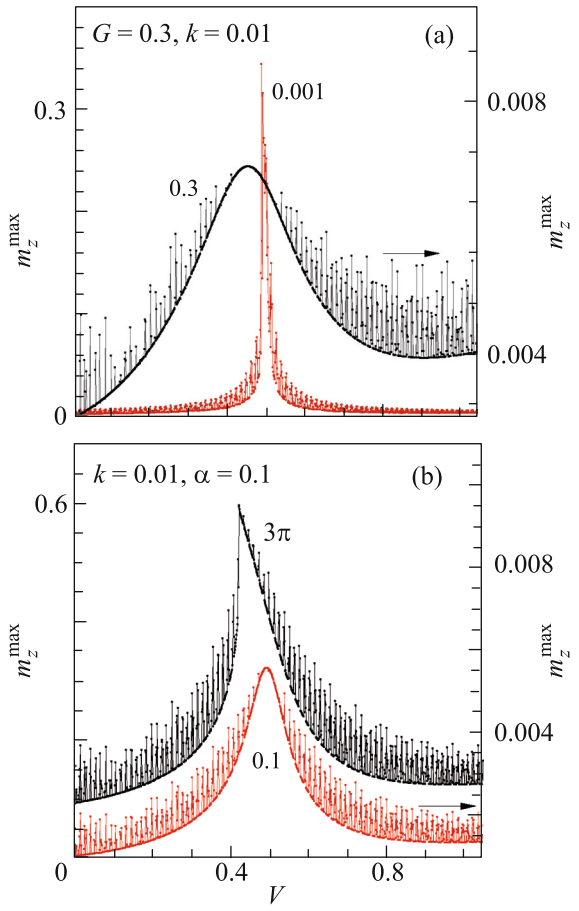

Fig. 2. (Color online) (a) Manifestation of the ferromagnetic resonance on the dependence $m_z^{max}(V)$. The Gilbert damping α is indicated. (b) Manifestation of the ferromagnetic resonance on the dependence $m_z^{max}(V)$ at two indicated ratios G of the Josephson energy to the energy of the nanomagnet; the effect of the ratio G on the width of the ferromagnetic resonance is seen.

$\alpha = 0.3$. The positions of peaks at weak damping are in good agreement with frequencies following from analytical formulas obtained by the linearization of the Landau–Lifshitz–Gilbert equations. In particular, if the deviation of the magnetic moment from the equilibrium direction caused by the interaction with the Josephson current is small, i.e., $G < 1$ and $k\tilde{m}_z < 1$, the Landau–Lifshitz–Gilbert equations can be linearized. In this case, the resonance frequency is given by the expression

$$\Omega_{Res} = \sqrt{\frac{-a_2 + \sqrt{a_2^2 - 4a_1}}{2a_1}}, \qquad (3)$$

where $a_1 = (\alpha^2 + \alpha k \Omega_F \epsilon + 1)^2$ and $a_2 = 2\alpha^2 + k^2\Omega_F^2\epsilon^2 + 2\alpha k\Omega_F\epsilon - 2$.

In particular, at $G = 0.3$, $k = 0.01$, and $\Omega_F = 0.5$, the resonance frequencies for $\alpha = 0.001$ and 0.3 are $\Omega_{Res} \approx 0.5$ and 0.45, respectively, which are fairly close to the values obtained numerically (see Fig. 2a).

The width of the resonance depends on the Gilbert damping parameter α, the ratio G of the Josephson energy to the energy of the nanomagnet, and the coupling parameter k. Figure 2b demonstrates the effect of the ratio G on the parameters of the ferromagnetic resonance. As the ratio G increases, the resonance frequency decreases and the resonance peak becomes asymmetric with respect to $\Omega_J = \Omega_F$. In this case, analytical expressions give $\Omega_{Res} \approx 0.492$ at $\alpha = 0.1$, $G = 0.1$, $k = 0.01$, and $\Omega_F = 0.5$. However, analytical results at $G = 3\pi$ are overestimated; this means that it is necessary to take into account higher order terms at $G \gg 1$. Thus, the deviation m_z in resonance can be quite large at certain G, k, and α values and can be manifested under experimental conditions.

Another interesting result of this work is the reorientation of the easy axis of the nanomagnet at an increase in the Josephson-to-magnetic energy ratio, i.e., a specific manifestation of the properties of the Kapitza pendulum in the "Josephson junction–nanomagnet" system. Figure 3 shows the dynamics of the magnetic moment component $m_z(t)$ at different G values. We emphasize that the magnetic moment at the initial time is directed along the easy axis (y axis). It is seen the component $m_z(t)$ at small G values with increasing time tends to a constant value depending on G. With an increase in G, this dependence changes significantly, and $m_z(t)$ at $G = 3\pi$ oscillates and tends to unity at large times; i.e., m_y vanishes. Thus, the easy axis of the nanomagnet is reoriented. The magnetic moment of the nanomagnet in intermediate states is oriented between the y and z axes. The time of reorientation decreases with increasing G.

Figure 4 shows the dynamics of the component m_z at various Ω_J values. It is seen that the component m_z at low Ω_J values precesses near a certain fixed value, whereas at large Ω_J values, it oscillates and approaches unity.

It is known that the stable equilibrium position of the pendulum changes if its point of suspension oscillates at a high frequency [16]. The Josephson-to-magnetic energy ratio G corresponds to the amplitude of a variable force in the problem of the Kapitza pendulum, which should promote the reorientation of the easy axis of the ferromagnet. The character of an increase in the average value of m_z as a function of the Josephson-to-magnetic energy ratio G is illustrated in Fig. 5, which also demonstrates analogy with the Kapitza pendulum. A similar behavior is observed at an increase in the coupling parameter k between the Josephson and magnetic subsystems.

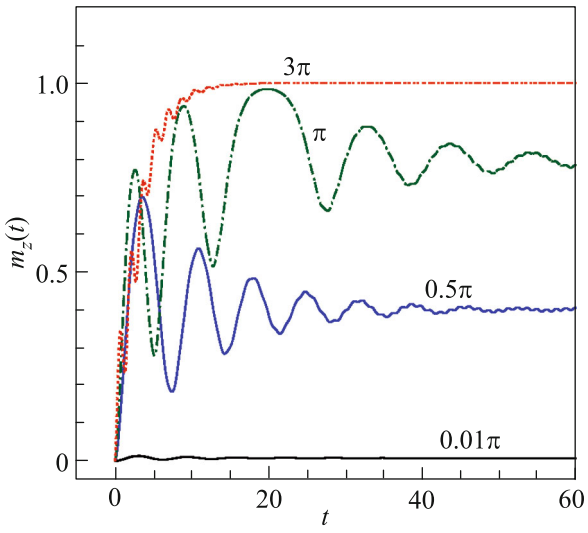

Fig. 3. (Color online) Dynamics of the magnetic field component m_z at four indicated G values for $k = 0.05$ and $\alpha = 0.1$.

We demonstrate the possibility of the flip of the magnetic moment under the action of the external current pulse. The equation relating the current pulse to the phase difference has the form

$$\frac{d\varphi}{dt} = I_{\text{pulse}} - \sin(\varphi - km_z) + k\frac{dm_z}{dt}. \qquad (4)$$

Here, the external current pulse is specified as

$$I_{\text{pulse}}(t) = \begin{cases} A_s, & t \in [t_0 - 1/2\Delta t, t_0 + 1/2\Delta t]; \\ 0, & \text{otherwise}, \end{cases} \qquad (5)$$

where A_s and Δt are the amplitude and duration of the current pulse, respectively. Equation (4) is solved numerically together with the system of equations (1) including the effective field (2). Note that Vt and V in Eqs. (1) and (2) are replaced by φ and $d\varphi/dt$, respectively. The results of the calculation are shown in Fig. 6. In contrast to [11] (Fig. 3), where flip was ensured by the specific variation of the voltage (linearly decreasing) in time, the flip time in the case of the current pulse is two orders of magnitude shorter, which is a significant advantage. We note that the parameters of the calculations are the same in both cases.

We consider above the effect of Josephson oscillations on the dynamics of the magnetic moment of the nanomagnet. We now briefly describe the inverse effect, i.e., the effect of the dynamics of the magnetic moment on the current–voltage characteristic of the Josephson junction [17]. The current–voltage characteristic is calculated for the junction with a given current. In this case, the system of equations within the

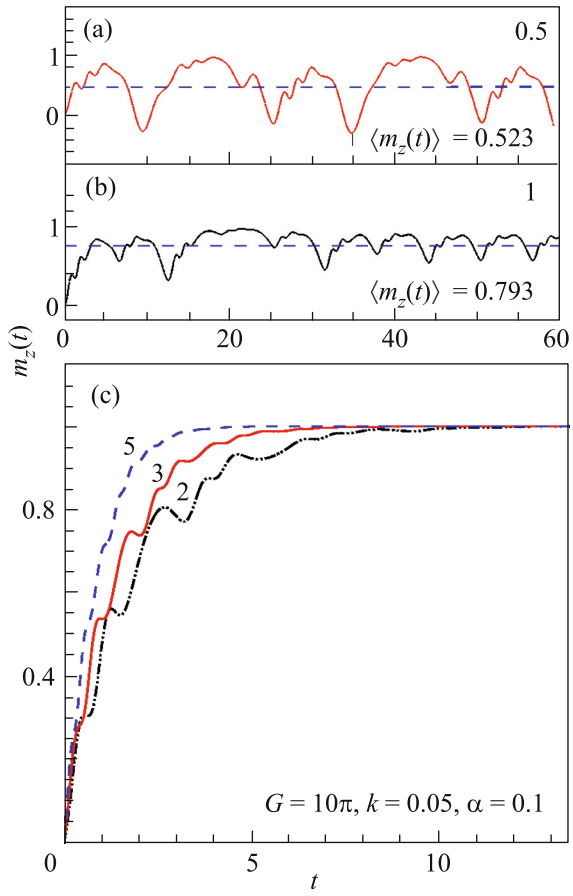

Fig. 4. (Color online) Dynamics of the magnetic field component m_z at Ω_J = (a) 0.5, (b) 1, and (c) 2, 3, and 5. The dashed line in panels (a) and (b) is the average value of the magnetic field component m_z.

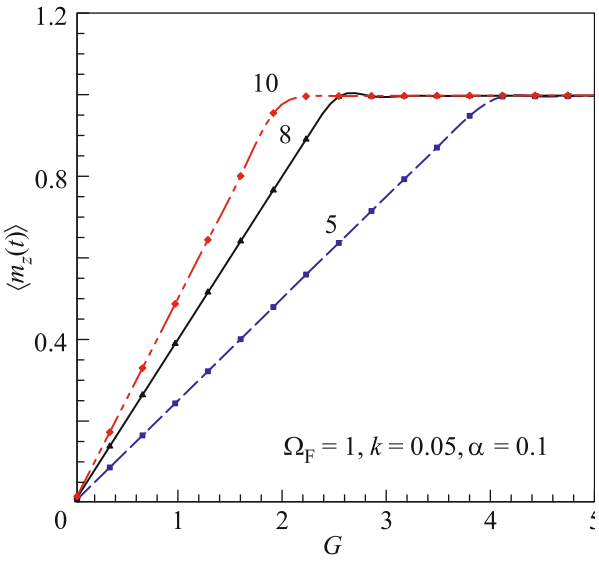

Fig. 5. (Color online) Average value of the magnetic field component m_z versus the Josephson-to-magnetic energy ratio G for three indicated Josephson frequencies.

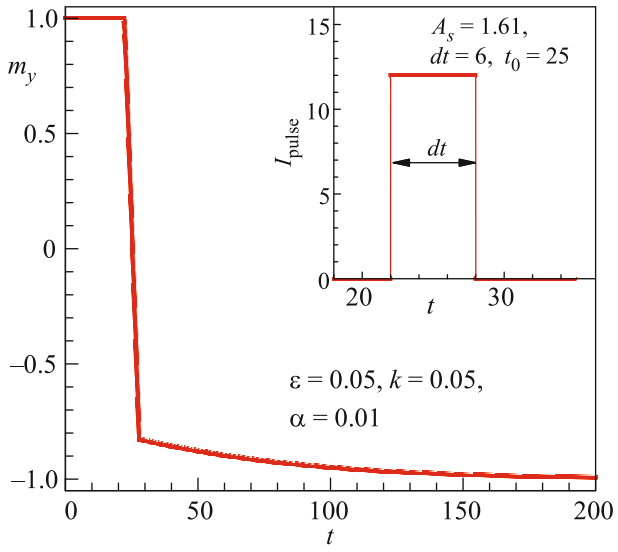

Fig. 6. (Color online) Demonstration of the flip of the magnetic field component m_y by the base current pulse. The inset shows the pulse shape.

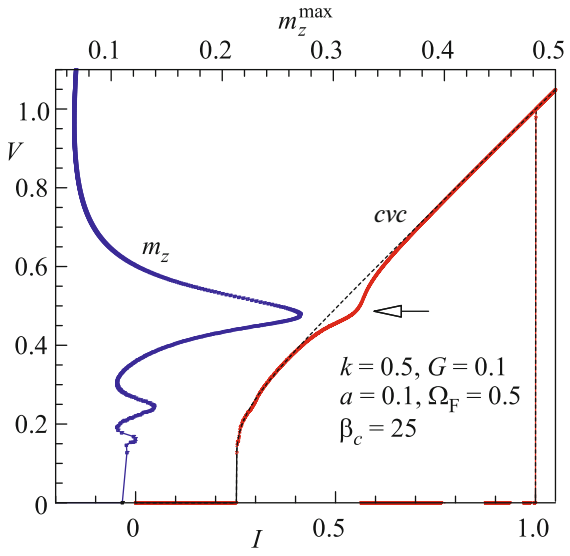

Fig. 7. (Color online) Current–voltage characteristic of the Josephson junction (solid line *cvc*) with and (dashed line) without the nanomagnet along with the voltage dependence of the maximum amplitude of the magnetic field component m_z.

resistively and capacitively shunted junction model has the form

$$\frac{dV}{dt} = \frac{1}{\beta_c}\left[I - \sin[\varphi - km_z] + V - k\frac{dm_z}{dt}\right], \qquad (6)$$

$$\frac{d\varphi}{dt} = V, \qquad (7)$$

where φ is the phase difference in the Josephson junction and β_c is the McCumber parameter. Furthermore, to calculate the current–voltage characteristic, *Vt* in Eqs. (1) and in expression (2) for the effective field should be replaced by φ.

The current–voltage characteristic of the Josephson junction with and without the nanomagnet (superconductor–insulator–superconductor junction) is shown in Fig. 7 together with the voltage dependence of the maximum component m_z and the calculation parameters. The current–voltage characteristic of the Josephson junction with the nanomagnet has a feature marked by the arrow, which is absent on the current–voltage characteristic of the Josephson junction without the nanomagnet. The voltage position of this feature corresponds to the position of the resonance peak of m_z. Thus, the precession of the nanomagnet is manifested on the current–voltage characteristic of the Josephson junction, which can be used to control its dynamics.

We justify the chosen parameter values. The results shown in Fig. 2a correspond to the parameters $G = 0.3$ and $k = 0.01$, which can be reached for the Josephson junction with an energy of 4.9×10^{-20} J and the nanomagnet that has a radius of 20 nm, a thickness of 6 nm, an anisotropy constant of 20 kJ/m^3, and a saturation magnetization of 1420 kA/m and is located at a distance of 300 nm. Close parameters were used in [20–23]. The parameters $G = 3\pi$ and $k = 0.05$ at which the easy axis of the nanomagnet is reoriented (Fig. 3) and the parameters $G = 0.05$ and $k = 0.05$ at which the component m_y of the nanomagnet is flipped (Fig. 6) are obtained for Josephson junctions with energies of 3.3×10^{-21} and 1.45×10^{-18} J, respectively, with the nanomagnet located at a distance of 65 nm. The presented estimates indicate that the results obtained in this work can be experimentally implemented. The justification of the parameters used in this work and their correspondence to experimental conditions were also discussed in [4, 11].

To summarize, we have studied the dynamics of the nanomagnet coupled to the Josephson junction and have revealed a number of interesting features of this dynamics. The precession of the magnetic moment caused by the superconducting current results in the ferromagnetic resonance. We have demonstrated that the easy axis of the nanomagnet is reoriented at an increase in the frequency of Josephson oscillations, the Josephson-to-magnetic energy ratio, and the coupling parameter between the Josephson current and magnetic moment.

At the same time, a number of properties of this system remain unstudied. In particular, the periodic impact on the nonlinear system can induce chaotic states [18]. Chaos induced in the Josephson junction by the external electromagnetic radiation, which is simulated by the term $A\sin\omega t$ added to the main term (ω and *A* are the frequency and amplitude of radiation,

respectively), was considered in detail in [19]. We suppose that the precession of the magnetic moment under the action of superconducting oscillations in the Josephson junction in the system under study can also induce chaotic states. Studies in this direction have not yet been performed but are certainly important for applications of these systems.

FUNDING

This work was supported by the Russian Foundation for Basic Research (project nos. 18-02-00318, 18-32-00950, and 18-52-45011). The numerical calculations were supported by the Russian Foundation for Basic Research (project no. 18-71-10095).

REFERENCES

1. A. Golubov and M. Yu. Kupriyanov, Nat. Mater. **16**, 156 (2017).
2. J. Linder and W. A. Jason Robinson, Nat. Phys. **11**, 307 (2015).
3. Yu. M. Shukrinov, I. R. Rahmonov, K. Sengupta, and A. Buzdin, Appl. Phys. Lett. **110**, 182407 (2017).
4. L. Cai, D. A. Garanin, and E. M. Chudnovsky, Phys. Rev. B **87**, 024418 (2013).
5. A. Buzdin, Phys. Rev. Lett. **101**, 107005 (2008).
6. F. Konschelle and A. Buzdin, Phys. Rev. Lett. **102**, 017001 (2009).
7. I. Zutic, J. Fabian, and S. Das Sarma, Rev. Mod. Phys. **76**, 323 (2004).
8. A. A. Golubov, M. Y. Kupriyanov, and E. Ilichev, Rev. Mod. Phys. **76**, 411 (2004).
9. A. I. Buzdin, Rev. Mod. Phys. **77**, 935 (2005).
10. S. Mai, E. Kandelaki, A. F. Volkov, and K. B. Efetov, Phys. Rev. B **84**, 144519 (2011).
11. L. Cai and E. M. Chudnovsky, Phys. Rev. B **82**, 104429 (2010).
12. P. K. Atanasova, S. A. Panayotova, E. V. Zemlyanaya, Yu. M. Shukrinov, and I. R. Rahmonov, Lect. Notes Comput. Sci. **11189**, 301 (2019).
13. K. K. Likharev, *Dynamics of Josephson Junctions and Circuits* (Gordon and Breach, London, 1986; Nauka, Moscow, 1985).
14. L. D. Landau and E. Lifshitz, Phys. Z. Sowjetunion **8**, 153 (1935).
15. T. L. Gilbert, IEEE Trans. Magn. **40**, 3443 (2004).
16. L. D. Landau and E. M. Lifshitz, *Course of Theoretical Physics,* Vol. 1: *Mechanics* (Nauka, Moscow, 1982; Pergamon, New York, 1988).
17. R. Ghosh, M. Maiti, Y. M. Shukrinov, and K. Sengupta, Phys. Rev. B **96**, 174517 (2017).
18. Yu. M. Shukrinov, A. E. Botha, S. Yu. Medvedeva, M. R. Kolahchi, and A. Irie, Chaos **24**, 033115 (2014).
19. R. L. Kautz and R. Monaco, J. Appl. Phys. **57**, 875 (1985).
20. P. Mangin and R. Kahn, *Superconductivity: Anintroduction* (Springer Int., Grenoble Sciences, Cham, Grenoble, 2017).
21. R. P. Cowburn, A. O. Adeyeye, and M. E. Welland, New J. Phys. **1**, 16 (1999).
22. L. F. Yin, D. H. Wei, N. Lei, L. H. Zhou, C. S. Tian, G. S. Dong, X. F. Jin, L. P. Guo, Q. J. Jia, and R. Q. Wu, Phys. Rev. Lett. **97**, 067203 (2006).
23. K. H. J. Buschow, *Concise Encyclopedia of Magnetic and Superconducting Materials* (Elsevier Science, Amsterdam, Netherlands, 2005).
24. Yu. M. Shukrinov, A. Mazanik, I. R. Rahmonov, A. E. Botha, and A. Buzdin, Europhys. Lett. **122**, 37001 (2018).

Translated by R. Tyapaev